IOPscience iopscience.iop.org

Home Search Collections Journals About Contact us My IOPscience

Dimensionality crossover in the induced magnetization of Pd layers

This article has been downloaded from IOPscience. Please scroll down to see the full text article.

2007 J. Phys.: Condens. Matter 19 246213

(http://iopscience.iop.org/0953-8984/19/24/246213)

View the table of contents for this issue, or go to the journal homepage for more

Download details:
IP Address: 129.252.86.83
The article was downloaded on 28/05/2010 at 19:14

Please note that terms and conditions apply.

IOP PUBLISHING JOURNAL OF PHYSICS: CONDENSED MATTER

J. Phys.: Condens. Matter **19** (2007) 246213 (7pp) doi:10.1088/0953-8984/19/24/246213

Dimensionality crossover in the induced magnetization of Pd layers

Martin Pärnaste[1], Moreno Marcellini[1], Erik Holmström[2], Nicolas Bock[2], Jonas Fransson[2], Olle Eriksson[1] and Björgvin Hjörvarsson[1]

[1] Department of Physics, Uppsala University, Box 530, 751 21 Uppsala, Sweden
[2] Theoretical Division, Los Alamos National Laboratory, Los Alamos, NM 87545, USA

E-mail: bjorgvin.hjorvarsson@fysik.uu.se

Received 30 January 2007, in final form 13 April 2007
Published 24 May 2007
Online at stacks.iop.org/JPhysCM/19/246213

Abstract

The magnetic ordering of a series of samples consisting of ultrathin Fe layers embedded in Pd was investigated using the magneto-optical Kerr effect. The samples consisted of a single Fe layer with nominal thickness $0.2 \leqslant d_{\mathrm{Fe}} \leqslant 1.6$ monolayers sandwiched between two 20 monolayer Pd layers. A dimensionality crossover from two dimensions to three dimensions occurs as d_{Fe} is increased from 0.4 to 1.0 monolayers. First-principles calculations were performed in order to determine the magnetic profile, and we used a spin-wave quantum well model for obtaining a qualitative description of the dimensionality crossover. The results clearly prove the existence of a dimensionality crossover in the induced magnetization, opening new routes for addressing the influence of extension on order.

The dimensionality aspects of magnetic and structural phase transitions represent one of the cornerstones of modern science. For magnetic systems, the spin dimensionality as well as the spatial extension determines the universality class, giving rise to a myriad of ordering phenomena on different length scales. Furthermore, there are transition regions not represented by any universality class with corresponding critical exponents, but representing something in between. For example, the thickness dependence of the critical exponents of thin magnetic films exhibit such a transition, in which the exponents are continuously varying with the thickness of the layers, from typical two-dimensional (2D) Ising ($\beta = 0.125$) to three-dimensional (3D) Heisenberg ($\beta \approx 0.36$) [1, 2] behaviour.

Experimental investigations of magnetic dimensionality are challenging, partly because of the difficulties of making samples with the intended properties. For example, imperfections such as atomic steps and other structural defects are always present in real samples. Even close to ideally layer-by-layer grown samples have imperfections due to incomplete formation of atomic layers, resulting in thickness variations as well as the presence of atomic steps. Atomic

 © 2007 IOP Publishing Ltd Printed in the UK

steps can result in locally preferred directions of the magnetization [3], giving rise to almost randomized anisotropy, influencing the order–disorder transition in an unpredictable way. The thickness variation originating from the incomplete formation of atomic layers will also inevitably give rise to a distribution with respect to the inherent ordering temperature. These limitations are minimized for ultrathin magnetic layers sandwiched between layers of materials with a long-range polarizability and high susceptibility. The idea is based on competition between the length scales involved. When the range of the induced magnetization is much larger than the length scale of the atomic imperfections, their influence will be negligible at some distance from the defect. Hence, as long as the range of the induced moment is large enough, near to perfect layered magnetization is conceivable.

The high magnetic susceptibility and long-range polarizability of Pd make it a suitable candidate for these studies. The Fe-induced magnetic moment in bulk Pd is large, e.g., a single Fe impurity in Pd polarizes a sphere of about 10 Å radius [4, 5] resulting in a total magnetic moment of 9–12 μ_B per Fe atom [6, 4, 7]. When the (Fe) dopants increase in density, a saturation of the Pd moment is observed [4]. The polarized region from a covered monolayer (ML) of Fe in Pd extends as far as 20 Å [5], or ∼10 ML [8]. This range is large with respect to imperfections at the atomic scale; hence, the influence of defects such as atomic steps is expected to be strongly damped.

Here we present experimental and theoretical investigations of the magnetic ordering in ultrathin Fe films sandwiched between two thicker Pd layers. We will discuss the influence of the concentration of Fe on the ordering temperature and dwell on the extension of the induced magnetization while addressing the dimensionality of the magnetic transition.

A series of ten samples was grown on MgO(100) substrates using DC magnetron sputtering. The Pd(20 ML)/Fe(d_{Fe}ML)/Pd(20 ML) structures were grown on 10 ML V seeding layers, slightly above room temperature. The thickness of the Fe layers was controlled by the timing of the deposition shutter, using a calibrated deposition rate of 0.107 ± 0.005 Å s^{-1}. The investigated range was $0.2 \leqslant d_{Fe} \leqslant 1.6$ ML, which can also be viewed as a change from dilute to continuous Fe layers.

The temperature-dependent magnetization was determined through the magneto-optical Kerr effect. Passive shielding of the ambient magnetic field was obtained by three mu-metal cylinders, resulting in a background field below 1 μT for the measurements of the remanent magnetization. Magnetic field was applied with a pair of Helmholtz coils placed within the magnetic shielding, allowing measurements in the field range ±8 mT. A detailed description of the set-up can be found in [9].

In the critical region, the magnetization versus temperature can be described by a power law

$$m \propto (-t)^{\beta}, \tag{1}$$

where the exponent β reflects the magnetic dimensionality [10] of the transition. Here the determination of the exponents is made using two methods. The first approach is a direct fitting of the data using equation (1), in which a (Gaussian) distribution of the critical temperature (T_c) is used to replicate the small finite-size tailing of the magnetization [11, 9]. The fitting yields T_c via the relation $t = (T - T_c)/T_c$, as well as the exponent β. The lower bound of the fitting range was fixed to $t = -0.2$. Typical broadening of $\sigma \approx 1$ K is obtained, assuming a Gaussian distribution of T_c. Using the mean value of T_c as derived from direct fitting, we plot the magnetization versus t on a double logarithmic scale, from which the exponent β is extracted as the linear slope; see figure 1. A true 2D XY system is critical for all temperatures below T_c [12]; hence the linearized range is a direct measure of the extension of the 2D criticality. A reduction of the extension of the critical region is observed with increasing Fe thickness for

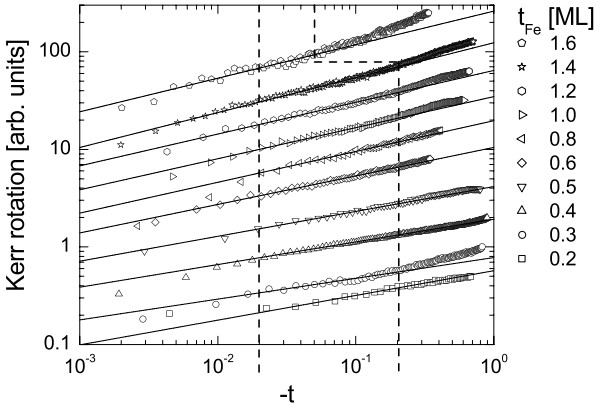

Figure 1. Magnetization versus reduced temperature. The straight lines in connection with each dataset represent the slope in the fitted interval (between the two dashed lines), i.e., the exponent β. The datasets are offset for clarity.

$d_{\mathrm{Fe}} \geqslant 0.8$ ML, as seen in figure 1. Due to the reduction of the critical region the data for the sample with $d_{\mathrm{Fe}} = 1.6$ ML were fitted in the interval $0.02 \leqslant (-t) \leqslant 0.05$, as compared to $0.02 \leqslant (-t) \leqslant 0.2$ for all other samples.

All samples are characterized by a Kerr rotation of opposite sign with respect to that of Fe [13, 14], which confirms that the measured magnetic signal is totally dominated by the induced Pd magnetization.

Figure 2 shows T_{c} versus d_{Fe} together with a linear fit, yielding a $\sim$200 K ML^{-1} slope. The increase of T_{c} with d_{Fe} is similar to that found in Co films deposited on Cu(100) substrates [16]. Apparently T_{c} varies close to linearly with d_{Fe} in the region $0.4 \lesssim d_{\mathrm{Fe}} \lesssim 1.5$ ML. This behaviour is in stark contrast to the observed power-law behaviour of T_{c} versus thickness in thin films, as reported by many authors [1, 17–19]. The changes in the ordering temperature also provide information on the confinement of the Fe layers. If the Fe were evenly distributed in the Pd layer, the ordering temperature would resemble that of a random alloy. The dashed line in figure 2 shows the expected increase in T_{c} for a random distribution of Fe, using the data from [15]. These results were confirmed by determination of the ordering temperature of Fe/Pd alloy films with different Fe concentrations. The stronger increase of T_{c} for the ultrathin samples therefore highlights the influence of the spatial distribution of the Fe atoms in the Pd matrix. In other words, if the intermixing of Fe in Pd were complete, the increase of T_{c} with d_{Fe} would be the same as that shown by the dashed line in figure 2. Additional confirmation of the confinement of the Fe layers was obtained by x-ray analysis of both the actual films and Fe/Pd superlattices grown in the same system under identical conditions.

Figure 3 shows the exponent β versus d_{Fe} for all samples, as extracted by the two methods described above. When d_{Fe} is below 0.5 ML the magnetic dimensionality is clearly 2D XY-like with β in the range 0.21–0.26 [20]. At thicknesses larger than 0.5 ML, β increases with increasing d_{Fe}, reaching typical 3D values at around 1 ML. The transition from 2D to 3D magnetic ordering happens over a minute interval in d_{Fe}, $\sim$0.5 ML. In comparison, Fe layers in, for example, superlattice structures of Fe and V are non-magnetic up to thicknesses $\approx$1.7 ML [9]. Also, a 3 ML Fe film, sandwiched between V layers, displays 2D magnetic behaviour, marked by an exponent $\beta \approx 0.23$ [21].

The observed crossover in dimensionality, starting at d_{Fe} as low as $\approx$0.5 ML, highlights the importance of the induced moment in Pd when defining the effective magnetic thickness. For

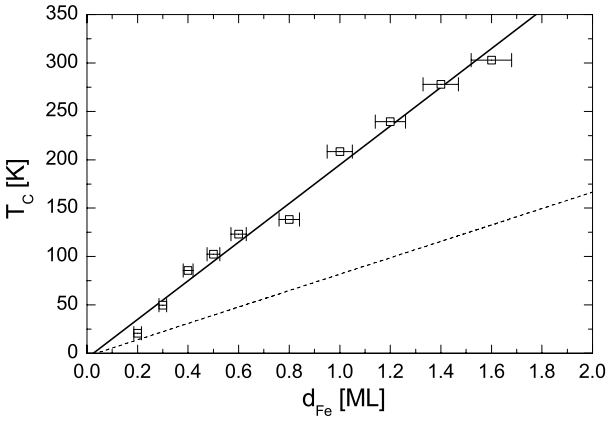

Figure 2. T_c versus d_{Fe} in this study. The full line represents a linear fit to the data with a slope $\sim$200 K ML^{-1}. The dashed line represents the increase of T_c for an Fe–Pd alloy, the slope being $\sim$85 K ML^{-1}. The alloy data are from [15].

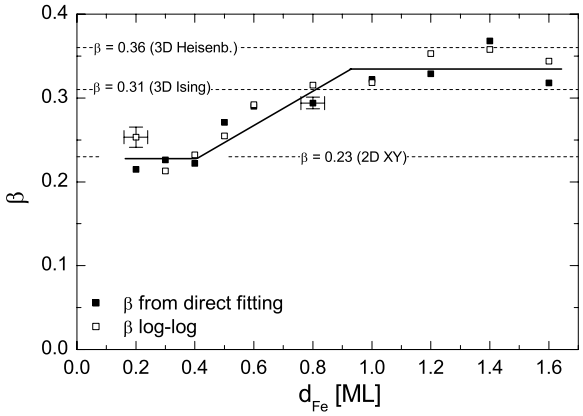

Figure 3. Exponent β versus d_{Fe} for all samples in this study, as determined by direct fitting and by double logarithmic plotting. The dashed horizontal lines represent β of the 2D XY, 3D Ising, and 3D Heisenberg models. The solid line serves as a guide to the eye. Typical uncertainties in β and thickness are indicated.

comparison, Li and Baberschke and later Huang *et al* determined the dimensionality crossover in Ni films on Cu and W substrates [1, 2] to be around 5–7 ML. Based on this comparison it is likely that the dimensionality crossover found here must be governed by the induced moment in Pd.

To explore the underlying causes for the changes in the dimensionality, we calculated the Fe-induced magnetic profile. The calculations were performed using a spin-polarized interface Green's function technique, based on the linear muffin-tin orbitals method within the tight-binding, frozen core and atomic sphere approximations, as developed by Skriver and Rosengaard [22]. The Fe–Pd samples were treated locally as an alloy within the coherent potential approximation [23–25]. Convergence was ensured for all calculations both with respect to total energy and k-space sampling. We found that 528 k-points in the irreducible part of the Brillouin zone were sufficient to obtain convergence in all the cases considered. The crystal structure was assumed to be fcc with the lattice constant of bulk Pd.

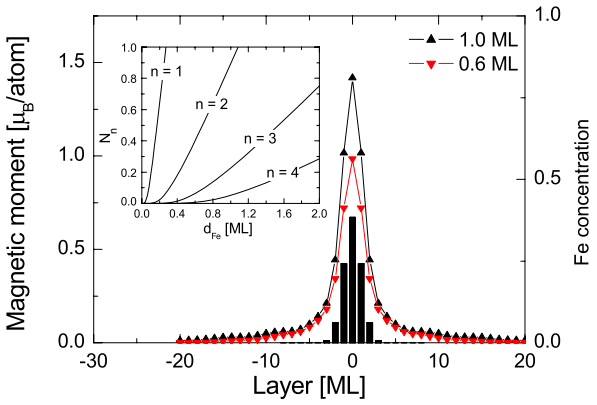

Figure 4. Calculated decay of the magnetic moment with increasing distance from the centre Fe layer (layer '0') for $d_{\mathrm{Fe}} = 0.6$ and 1.0 ML. The barsrepresent the distribution of the Fe layer used in the model. Inset: occupation number of magnons in the out-of-plane direction, at T_{c}, versus d_{Fe} for the four lowest magnon modes.

(This figure is in colour only in the electronic version)

To include structural imperfections such as atomic steps and interdiffusion in the theoretical analysis, the Fe layers are treated as an alloy. This approach decreases problems associated with interference terms in the calculations, arising from the finiteness of the structures. The spatial extent of the interface alloy at an A/B interface in a sample can be described by a Gaussian distribution function with standard deviation Γ. Since the actual distribution is unknown it is reasonable to assume a Gaussian form based on the central limit theorem. The layer-dependent concentration profile around the A/B interface is obtained as an integral over this distribution. The total concentration profile of the trilayer is obtained as a sum over the A/B and B/A interface profiles in the sample; for more details see [26] and [27].

The results are illustrated in figure 4, in which the moment at different distances from the central magnetic Fe layer, denoted as layer '0', for $d_{\mathrm{Fe}} = 0.6$ and 1.0 ML is plotted. The magnetization profiles are calculated using $\Gamma = 1.0$ ML. The moment of the Fe-containing layer increases, as expected, with increasing Fe content. The increase in T_{c} with increasing amount of Fe is thereby understandable as resulting from an increase in the effective magnetic coupling. Thus, a conceptual picture of the increasing T_{c} emerges; however, the results do not yield any understanding of the dimensionality crossover in the actual thickness range. The magnetic profile appear to be rather insensitive to the amount of Fe. To understand this, we need to discuss how the amplitude and the extension of the magnetic profile affect magnetic excitations.

The different components of the magnetic excitations may be analysed within a simple quantum well model, based on the ideas behind the anisotropic Heisenberg model. The main idea is based on the separation of the in-plane (XY) and the out-of-plane (Z) contributions to the magnetic excitations. The spatial confinement (see figure 4) in the Z-direction will lead to discrete energy levels of the magnetic excitations (magnons) with relatively high energy levels as compared to the XY modes. The dimensional crossover can be regarded as reflecting the relative population of these principal modes in the vicinity of the ordering temperature. For thicknesses below $d_{\mathrm{Fe}} \approx 0.4$, the contribution from Z-magnon modes would be minute up to T_{c}, resulting in 2D XY-like behaviour. Consequently, the increase in T_{c} with increasing d_{Fe} allows the population of Z-magnon modes, eventually resulting in 3D-like behaviour.

The main concern here is therefore to explore the changes in the contribution of the Z-magnon modes to the magnetic excitations of the samples with different T_c. Thus, the probability of the excitation of modes in the Z-direction will serve as a marker for the dimensionality of the transition. We use the fact that $T_c \propto d_{Fe}$ and set the effective width of the quantum well, somewhat arbitrarily, to $W = 11$ ML, since only within the central ∼11 ML is there a noticeable difference between samples with different d_{Fe}. The energy levels are then given by $E_n \propto k_n^2$, where n is the quantum number, $k_n = (n\pi/W)$ is the wavevector and the available energy is $k_B T_c$. $E \propto k^2$ is a valid approximation for small k of the common $E \propto [1 - \cos(ka)]$ expression for magnon dispersion. The proportionality constant is determined by the spin-stiffness of the magnetic layers. In these samples, both the local concentration of Fe and the magnetic moment vary with position, which makes the modelling of the spin-stiffness non-trivial to implement. We have chosen to approximate the varying spin-stiffness with a constant value, calculated by fixing the atomic magnetic moment of Pd locally to 0.1 μ_B. Thereafter we calculated the spin spiral spectrum and extracted the spin-stiffness constant, using the method outlined by Rosengaard and Johansson [28]. Using the energy relation for the magnons as calculated from the approximate stiffness constant and the Planck distribution for the magnon occupation, we can express the population of the nth mode, at T_c, as

$$N_n = \left[\exp\left(\frac{D\pi^2 n^2}{W^2(a/2)^2 c k_B d_{Fe}}\right) - 1\right]^{-1} \approx \left[\exp\left(\frac{0.188 n^2}{d_{Fe}}\right) - 1\right]^{-1}, \qquad (2)$$

where $D = 150$ meV Å^2 is the spin-stiffness, $a = 3.89$ Å is the lattice constant for Pd, and $c = 200$ K ML^{-1} is the proportionality constant for T_c versus d_{Fe}.

The resulting occupation numbers for the first four modes are shown in the inset of figure 4. It may be seen that the dimensionality crossover of the induced moment can indeed be understood as a relative increase of the population of the Z-magnon modes. Following this line of argument, the Z-magnon modes are not populated up to T_c for small thicknesses, yielding a 2D XY-like behaviour. With increasing T_c (d_{Fe}) the magnon modes start to become significantly occupied, contributing to the overall magnetic excitations and eventually yielding a shift of the effective exponent β.

As can be seen in the inset of figure 4, the occupation of higher-order Z-magnon modes is negligible up to T_c when d_{Fe} is below a critical thickness (0.4 ML). Above this thickness the occupation rises rapidly with increasing d_{Fe}, which can be interpreted as the beginning of the dimensional crossover. Several magnon modes become accessible within a small thickness range, which eventually leads to 3D behaviour of the magnetization. A qualitative picture of the sharp dimensionality crossover at $d_{Fe} = 0.5$–1.0 ML is thereby obtained.

The ultrathin Fe layers used to polarize the surrounding Pd may be viewed as magnetic δ-doping. The effects discussed here can therefore be viewed as the magnetic analogue to electronic doping in semiconductors. The heuristically based explanation of the changes in the induced magnetization is plausible and actually quite close to the model discussed in [29]. However, the simplifications we make in the theoretical treatment do not allow quantitative analysis of many of the relevant parameters, such as the magnetic dispersion. Refinements of the theoretical and experimental approaches are therefore required to explore the influence of finite size and confinement on the ordering in finite systems.

Acknowledgments

Financial support from the Swedish Research Council (VR) and SSF is acknowledged. MP, MM, and BH also would like to thank P C W Holdsworth and S T Bramwell for valuable input during the preparation of this paper.

References

[1] Li Y and Baberschke K 1992 *Phys. Rev. Lett.* **68** 1208
[2] Huang F, Kief M T, Mankey G J and Willis R F 1994 *Phys. Rev.* B **49** 3962
[3] Kawakami R K, Escorcia-Aparicio E J and Qiu Z Q 1996 *Phys. Rev. Lett.* **77** 2570
[4] Low G G and Holden T M 1966 *Proc. Phys. Soc.* **89** 119
[5] Cheng L, Altounian Z, Ryan D H, Ström-Olsen J O, Sutton M and Tun Z 2004 *Phys. Rev.* B **69** 144403
[6] Craig P P, Nagle D E, Steyert W A and Taylor R D 1962 *Phys. Rev. Lett.* **9** 12
[7] Nieuwenhuys G J 1975 *Adv. Phys.* **24** 515
[8] Holmström E, Nordström L and Niklasson A M N 2003 *Phys. Rev.* B **67** 184403
[9] Pärnaste M, van Kampen M, Brucas R and Hjörvarsson B 2005 *Phys. Rev.* B **71** 104426
[10] Binney J J, Dowrick N J, Fisher A J and Newman M E J 1998 *The Theory of Critical Phenomena—An Introduction To the Renormalization Group* (Oxford: Oxford Science Publications)
[11] Elmers H J, Hauschild J and Gradmann U 1996 *Phys. Rev.* B **54** 15224
[12] Bramwell S T, Christensen K, Fortin J-Y, Holdsworth P C W, Jensen H J, Lise S, López J M, Nicodemi M, Pinton J F and Sellitto M 2000 *Phys. Rev. Lett.* **84** 3744
[13] Yaresko A N, Uba L, Uba S, Perlov A Ya, Gontarz R and Antonov V N 1998 *Phys. Rev.* B **58** 7648
[14] Zvezdin A K and Kotov V A 1997 *Modern Magnetooptics and Magnetooptical Materials* (Bristol: Institute of Physics Publishing)
[15] Büscher C, Auerswald T, Scheer E, Schröder A, Löhneysen H v and Claus H 1992 *Phys. Rev.* B **46** 983
[16] de Miguel J J, Cebollada A, Gallego J M, Miranda R, Schneider C M, Schuster P and Kirschner J 1991 *J. Magn. Magn. Mater.* **93** 1–9
[17] Ballentine C A, Fink R L, Araya-Pochet J and Erskine J L 1990 *Phys. Rev.* B **41** 2631
[18] Elmers H J and Gradmann U 1990 *Appl. Phys.* A **51** 255
[19] Bergholtz R and Gradmann U 1984 *J. Magn. Magn. Mater.* **45** 389
[20] Bramwell S T and Holdsworth P C W 1993 *J. Phys.: Condens. Matter* **5** L53–9
[21] Pärnaste M, Marcellini M and Hjörvarsson B 2005 *J. Phys.: Condens. Matter* **17** L477–83
[22] Skriver H L and Rosengaard N M 1991 *Phys. Rev.* B **43** 9538
[23] Soven P 1967 *Phys. Rev.* **156** 809
[24] Abrikosov I A and Skriver H L 1993 *Phys. Rev.* B **47** 16532
[25] Gyorffy B L 1972 *Phys. Rev.* B **5** 2382
[26] Holmström E, Nordström L, Bergqvist L, Skubic B, Hjörvarsson B, Abrikosov I A, Svedlindh P and Eriksson O 2004 *Proc. Natl Acad. Sci.* **101** 4742–5
[27] Holmström E 2003 Magnetism and structure in metallic multilayers *PhD Thesis* Uppsala Universitet
[28] Rosengaard N M and Johansson B 1997 *Phys. Rev.* B **55** 14975
[29] Mandal K, Mitra S and Kumar P A 2006 *Europhys. Lett.* **75** 618–23